

A high-throughput screening for inhibitors of riboflavin synthase identifies novel antimicrobial compounds to treat brucellosis

María Inés Serer¹, Mariela del Carmen Carrica^{1,†}, Jörg Trappe², Sandra López Romero², Hernán Ruy Bonomi^{1,‡}, Sebastián Klinke^{1,3}, María Laura Cerutti^{1,3} and Fernando Alberto Goldbaum^{1,3}

1 Fundación Instituto Leloir, IIBBA-CONICET, Buenos Aires, Argentina

2 Novartis Institutes for BioMedical Research, Basel, Switzerland

3 Plataforma Argentina de Biología Estructural y Metabólica PLABEM, Buenos Aires, Argentina

Keywords

brucellosis; drug development; flavin synthesis; high-throughput screening; riboflavin synthase

Correspondence

F. A. Goldbaum, Fundación Instituto Leloir, IIBBA-CONICET, Av. Patricias Argentinas 435 (C1405BWE) Buenos Aires, Argentina
Tel: +54-11-5238-7500
E-mail: fgoldbaum@leloir.org.ar
Website: www.leloir.org.ar/goldbaum-en

Present addresses

[†]Centro de Investigación y Desarrollo en Fermentaciones Industriales, CINDEFI-CONICET, Facultad de Ciencias Exactas, Universidad Nacional de La Plata, Argentina

[‡]Centre de Biochimie Structurale, CNRS UMR5048, INSERM U1054, Université de Montpellier, France

María Inés Serer and Mariela del Carmen Carrica contributed equally to this work.

(Received 11 January 2019, revised 26 February 2019, accepted 29 March 2019)

doi:10.1111/febs.14829

Brucella spp. are pathogenic intracellular Gram-negative bacteria adapted to life within cells of several mammals, including humans. These bacteria are the causative agent of brucellosis, one of the zoonotic infections with the highest incidence in the world and for which a human vaccine is still unavailable. Current therapeutic treatments against brucellosis are based on the combination of two or more antibiotics for prolonged periods, which may lead to antibiotic resistance in the population. Riboflavin (vitamin B₂) is biosynthesized by microorganisms and plants but mammals, including humans, must obtain it from dietary sources. Owing to the absence of the riboflavin biosynthetic enzymes in animals, this pathway is nowadays regarded as a rich resource of targets for the development of new antimicrobial agents. In this work, we describe a high-throughput screening approach to identify inhibitors of the enzymatic activity of riboflavin synthase, the last enzyme in this pathway. We also provide evidence for their subsequent validation as potential drug candidates in an *in vitro* brucellosis infection model. From an initial set of 44 000 highly diverse low molecular weight compounds with drug-like properties, we were able to identify ten molecules with 50% inhibitory concentrations in the low micromolar range. Further *Brucella* culture and intramacrophagic replication experiments showed that the most effective bactericidal compounds share a 2-Phenylamidazo[2,1-b][1,3]benzothiazole chemical scaffold. Altogether, these findings set up the basis for the subsequent lead optimization process and represent a promising advancement in the pursuit of novel and effective antimicrobial compounds against brucellosis.

Introduction

Brucellosis is one of the major zoonotic infections worldwide, causing devastating economic losses to the livestock industry and deleterious effects in humans

[1–3]. It is caused by the pathogenic intracellular Gram-negative bacteria *Brucella* spp. and is transmitted to humans through direct contact with infected

Abbreviations

HTS, high-throughput screening; LS, lumazine synthase; RS, riboflavin synthase.

animals or by consumption of infected, unpasteurized animal-derived products. The disease is essentially endemic in marginalized populations in low-income countries, reason why the World Health Organization has recently classified it as a neglected zoonotic disease [4].

With an estimated rate of 500 000 infections per year [5], there is still no available vaccine against human brucellosis. Current recommended antibiotic treatments involve prolonged administration regimens with two or more antimicrobial drugs to prevent relapses, which can cause undesired side effects on the patients and lead to antibiotic resistance in the population [2,6]. In addition, brucellosis may be complicated by life-threatening conditions such as endocarditis, neurobrucellosis or osteoarticular infections, which may require even longer or more aggressive therapeutic treatments [7,8]. Therefore, to deal with all these issues, there is a need for the development of new and effective antimicrobials against brucellosis.

Riboflavin (vitamin B2) is the precursor for the biosynthesis of flavin mononucleotide and FAD [9], two key redox cofactors involved in a variety of cellular metabolic processes [10]. While bacteria, plants, and fungi are able to biosynthesize riboflavin, humans and animals must obtain it from their diet, positioning riboflavin biosynthetic enzymes and regulatory factors as promising specific targets for antimicrobial therapies [11]. In fact, riboflavin biosynthesis has been shown to be essential in many pathogenic bacteria that lack riboflavin transporters, such as *Mycobacterium tuberculosis*, *Brucella abortus* and some *Salmonella* and *Escherichia* species [12–16].

The biosynthetic riboflavin pathway has been described in detail [9,17–19]. Lumazine synthase (LS, EC database: 2.5.1.78) catalyzes the penultimate step, allowing the condensation of 5-amino-6-ribitylamino-2,4 (1*H*,3*H*)-pyrimidinedione with 3,4-dihydroxy-2-butanone-4-phosphate to generate 6,7-dimethyl-8-ribityllumazine. Riboflavin synthase (RS, EC database: 2.5.1.9) catalyzes the last step, which corresponds to the dismutation of two molecules of 6,7-dimethyl-8-ribityllumazine (**a** and **b**) to yield one molecule of riboflavin **c**, with the regeneration of one molecule of 5-amino-6-ribitylamino-2,4 (1*H*,3*H*)-pyrimidinedione **d** (Fig. 1A).

Our laboratory has studied in detail these enzymes from *B. abortus*. For the former, we have identified two isoenzymes (RibH1 and RibH2/BLS) and characterized their tertiary and quaternary structures as well as their biochemical properties [20,21]. We have also assayed the relevance of the RibH enzymes in bacterial infection and demonstrated that the presence of at least one functional LS enzyme is essential for

intracellular survival and that RibH2/BLS is necessary for mice colonization. Moreover, RibH2/BLS constitutes a major candidate for the development of a subunit vaccine against brucellosis [14,22–24]. On the other hand, RS has been proposed as another important immunogenic candidate protein for the development of a brucellosis subunit vaccine [25]. More recently, our group has described the crystallographic structure of RS, both as apo-protein and in complex with a few ligands of interest, namely one of the products of the reaction (riboflavin) and two product analogues [roseoflavin and 5-nitro-6-ribitylamino-2,4 (1*H*,3*H*)-pyrimidinedione], which lead to the description of its active site (Fig. 1B) [26].

The structure-based design and synthesis of compounds with inhibitory activity against LS and RS have long been studied [27–36]. However, those compounds are very polar and thus not suitable for drug development. Interestingly, a high-throughput screening (HTS) hit compound targeting *M. tuberculosis* RS demonstrated antibiotic activity *in vitro*, although an off-target effect could not be totally discarded [37]. We here describe the development of a HTS assay for the identification of compounds with inhibitory activity against *Brucella* spp. RS and validate them in an *in vitro* model of brucellosis infection. We have identified a series of five hit compounds with drug-like properties sharing a common 2-Phenylamidazo[2,1-*b*][1,3] benzothiazole (PABT) chemical scaffold. These compounds also displayed *in vivo* bactericide activity against *B. abortus* and impaired bacterial replication in macrophagic cells. These results constitute a promising starting point for the rational design of effective drugs against brucellosis and other relevant infectious diseases.

Results

Development of a mobility shift-based screening assay (MSA) for RS inhibitors

We developed a mobility shift-based screening assay (MSA) based on the competitive binding of both riboflavin and inhibitor compounds to the active site of the enzyme. The screening uses microfluidic technology and is based on the differential migration of substrate and product in an electrophoretic separation. Thus, the presence of compounds with RS inhibitory activity was detected as a decrease in the fluorescence signal of riboflavin.

The MSA primary screening was performed over a highly diverse library of 44 000 low molecular weight (MW) compounds with drug-like properties. This

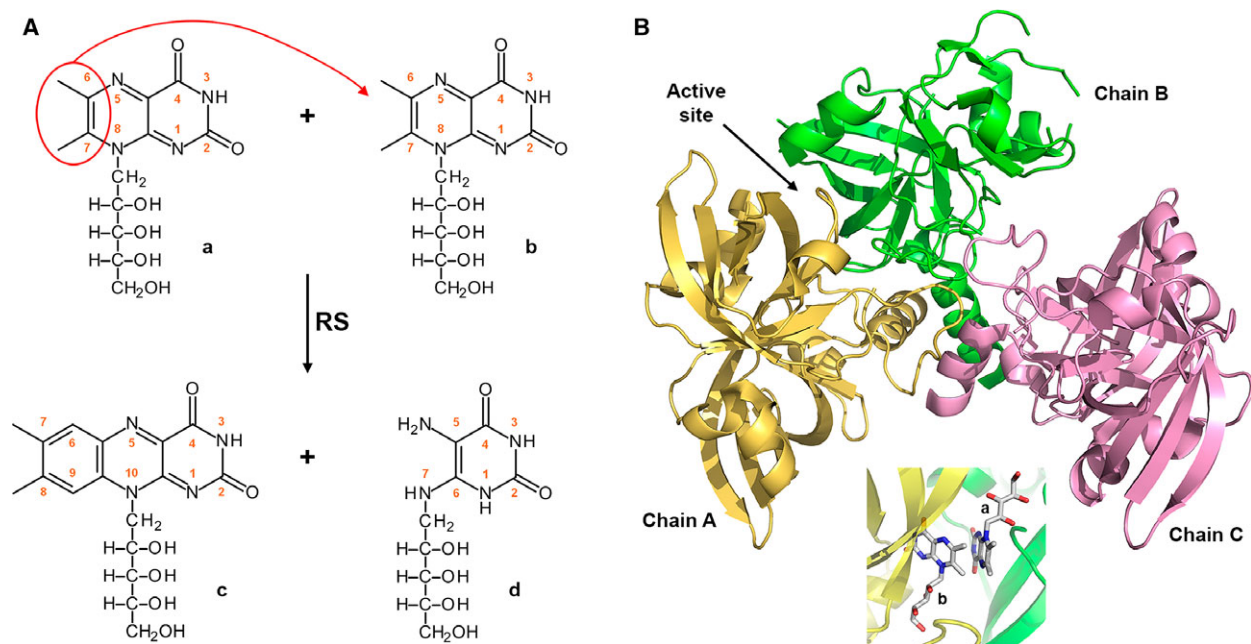


Fig. 1. RS catalysis and structure. (A) Reaction catalyzed by RS. A donor 6,7-dimethyl-8-ribyllumazine molecule **a** transfers a four carbon atom moiety to an acceptor 6,7-dimethyl-8-ribyllumazine molecule **b** generating riboflavin **c** and the side product 5-amino-6-ribylamino-2,4 (1*H*,3*H*)-pyrimidinedione **d**. (B) Crystal structure of *Brucella abortus* RS (as apo enzyme) determined by our group (PDB: 4FXU) [26]. The inset shows a model of the putative location of the substrate molecules in the active site.

screening was run under initial velocity conditions previously determined by both HPLC and the microfluidic system (Figs 2 and 3). A fluorescent peptide (JAK3) was used as an internal standard to compensate for the weak fluorescence of the substrate and to quantify product formation. A primary output of the run is shown in Fig. 4 as an example. The assay was developed in an off-chip mode and at a single compound concentration of 30 μM . As the hit calling criterion, the threshold value was set to 30% inhibition, resulting in a total of 163 hits (Fig. 5). Subsequently, the primary screening was validated by determining 50% inhibitory concentrations (IC_{50}) values by performing dose–response curves. Table 1 shows the 10 most potent compounds found by this approach. The IC_{50} values range between 2 and 32 μM , with IA-79-AF08 (inhibitor **1**) being the most potent with an IC_{50} of 2.4 μM . The dose–response curves obtained for IA-79-AF08 and the other selected compounds are shown in Fig. 6.

Structural analysis of the hits

The chemical structures of the 10 compounds with the highest RS inhibitory activities in the dose–response secondary screening are shown in Fig. 7. According to

their structure, these molecules can be clustered into two groups. The first group, which is presented in the upper row of Fig. 7 (inhibitors **4**, **5**, **6**, **9**, and **10**), comprise compounds that share a common chemical scaffold, namely a 2-PABT core formed by a heteroaromatic system of three rings linked to a phenyl group and two principal substituents: an alkyl or ethoxide group at position R1 and an aliphatic group with a terminal tertiary amine at position R2 (Fig. 8). On the other hand, the bottom row of Fig. 7 shows the rest of the studied compounds (inhibitors **1**, **2**, **3**, **7**, and **8**), without major chemical similarities, and which includes the most potent of the *in vitro* series, namely IA-79-AF08.

Nowadays, the probability of a small molecule to become an effective drug is established by the Lipinski ‘rules of five’ and other criteria that evaluate the physicochemical properties of the compounds according to: (a) $\text{MW} \leq 500$ Da; (b) lipophilicity index $\text{clogP} \leq 5$; (c) number of hydrogen bond acceptors (HBA) ≤ 10 ; (d) number of hydrogen bond donors (HBD) ≤ 5 ; (e) number of rotatable bonds (nRot) ≤ 10 and (f) the bioavailability descriptor topological polar surface area (tPSA) $< 140 \text{ \AA}^2$ [38–41]. A comprehensive analysis of the physicochemical properties of the selected hits revealed that, while compounds **1**, **2**, **7**, and **8**

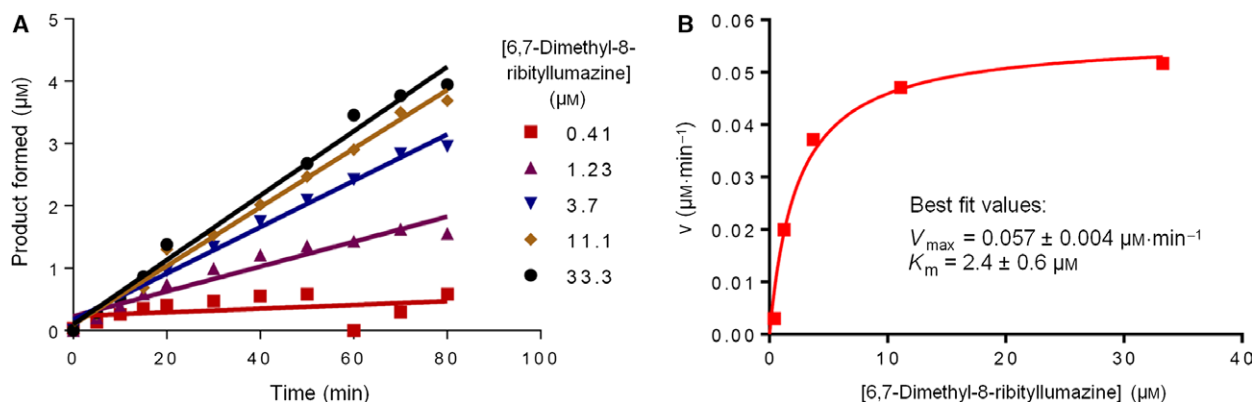


Fig. 2. Determination of the K_m value for 6,7-dimethyl-8-ribyllumazine by HPLC. (A) RS (8 nM) was incubated with serial dilutions of the 6,7-dimethyl-8-ribyllumazine substrate (0–100 μM) and reactions were stopped at different times during 80 min at RT. Product formation was quantified using a riboflavin standard curve. (B) K_m determination by curve fitting at $t = 80$ min.

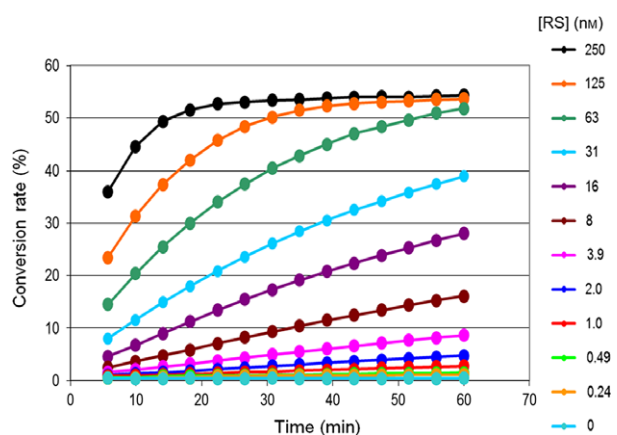


Fig. 3. Enzymatic generation of riboflavin in the MSA format. The conversion rate is shown for different RS concentrations. The optimal enzyme concentration chosen for the HTS was 8 nM.

presented slightly higher values in some of the properties, the PABT subset fulfilled the criteria established for drug-like candidates (Table 2). In particular, the PABT compounds presented lower tPSA values ($< 90 \text{ \AA}^2$), suggesting that they might display higher membrane passive diffusion rates *in vivo* [42].

Inhibition of *B. abortus* growth in culture

The inhibition of the RS activity *in vivo* is expected to abolish the capacity of *Brucella* to grow in a regular medium that does not contain high amounts of riboflavin. Thus, we evaluated whether the 10 selected RS inhibitors had an antibacterial effect on *B. abortus* on liquid cultures. We observed that the five compounds of the PABT subset were effective in decreasing the

bacterial growth throughout the entire duration of the experiment (Fig. 9A). Remarkably, cultures treated with inhibitor **4**, **6** or **10** completely abolished bacterial growth. On the other side **1**, the compound that showed the highest *in vitro* inhibition activity on RS, was unable to inhibit *Brucella* growth. This observation may be due to the fact that inhibitor **1**, along with **2**, **7**, and **8**, have higher tPSA values that could correlate with a reduced permeability to cross the bacterial membrane.

In order to determine the inhibitory potency of each of the compounds of the PABT subset, dose–response curves on *B. abortus* cultures were performed. Figure 9B shows that the observed inhibitory effect of the PABT compounds is concentration dependent. The IC_{50} values range from 27.9 to 85.7 μM , being compounds **4** and **10** the ones with the lowest IC_{50} values (Table 1).

Considering that the OD_{600} measurements do not allow discerning whether these compounds exert a bactericidal or a bacteriostatic effect, we subsequently evaluated whether the PABT compounds can affect the ability of *Brucella* to generate colony-forming units (CFU). For this purpose, *B. abortus* cultures were treated with the three PABT compounds that showed the highest potency in liquid cultures and the CFUs after 24 h of incubation were determined. Bacteria treated with inhibitors **4**, **6**, and **10** showed a decrease in 4.5, 2.9, and 2.7 log units in CFU per mL with respect to the initial culture, respectively (Fig. 9C). As expected for a 24 h *Brucella* culture, the DMSO control showed an increment of ~ 4.0 log units in CFU per mL relative to the inoculum (Fig. 9C). Altogether, these results demonstrate that the PABT compounds can exert a bactericidal effect on *B. abortus*.

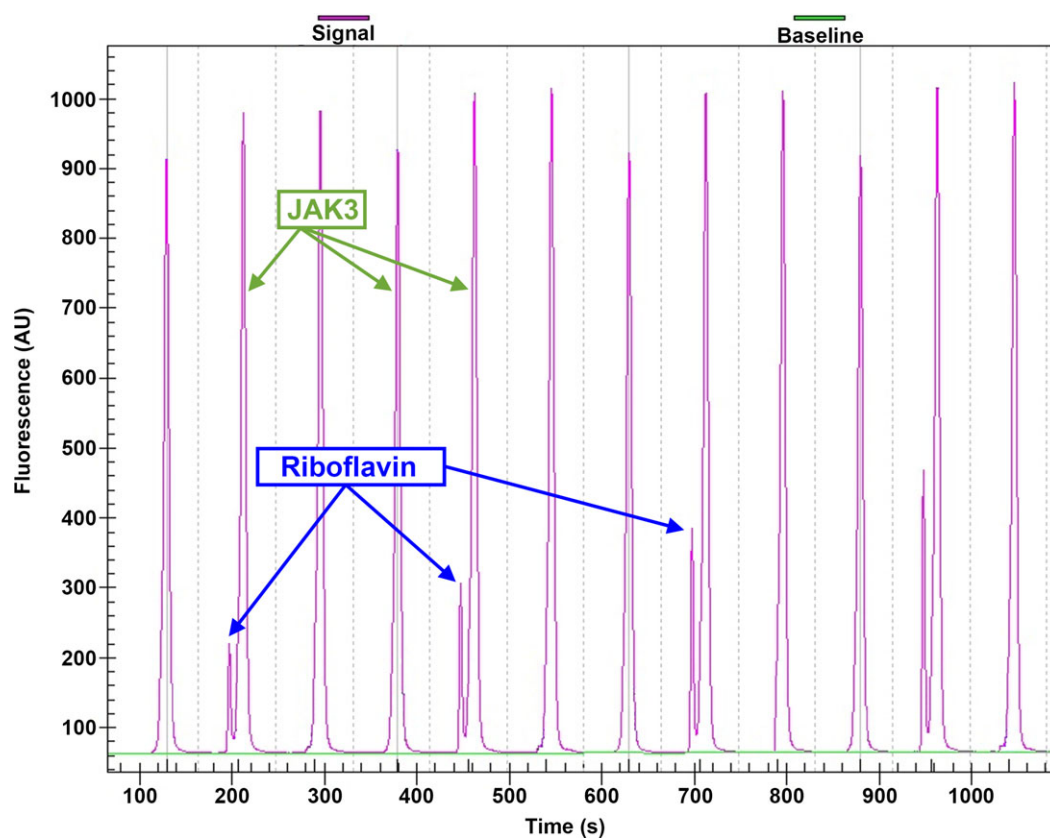


Fig. 4. Representative illustration of the primary output of the detection system. The RS activity was calculated from the areas of the product and substrate peaks in the presence of an internal fluorescent peptide standard (JAK3).

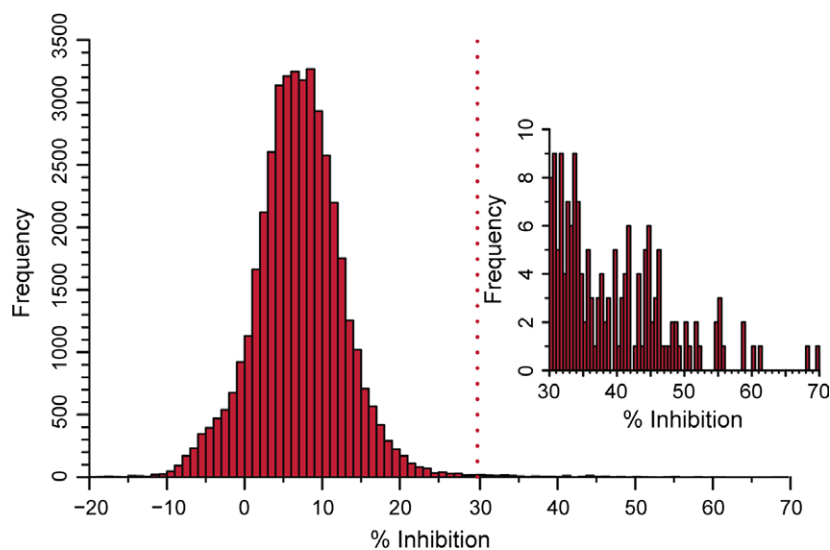


Fig. 5. MSA primary screening for *Brucella abortus* RS inhibitors. Distribution frequency of the 44 000 compounds tested for inhibitory activity. The HTS library was screened at a single concentration of 30 μM . The cut-off value was set at 30% inhibition (dotted line). Inset, zoomed view of the 163 unique hit compounds selected from this assay.

***In vivo* RS specific targeting by the PABT compounds**

Although the experiments described above successfully proved the inhibitory activity of the PABT compounds

on *B. abortus* growth, they did not demonstrate whether this effect is in fact associated with the inhibition of riboflavin biosynthesis. To rule out off-target effects, *B. abortus* was grown in tryptic soy broth (TSB) medium supplemented with riboflavin or 6,7-

Table 1. *In vitro* and *in vivo* effect of the 10 selected inhibitor compounds (sorted by IC₅₀ value in RS inhibition in ascending order). nd, not determined.

Compound commercial name	Compound number	IC ₅₀ (μM) (RS inhibition)	IC ₅₀ (μM) (Bacterial growth inhibition) ^a
IA-79-AF08	1	2.35	nd
OA-70-DS97	2	19.12	nd
YC-52-NV98	3	19.15	nd
QF-00-MV19	4	25.64	44.7
SC-03-QQ19	5	26.38	76.0
GF-00-MG19	6	27.80	54.7
IF-03-LB24	7	29.64	nd
UF-56-IL24	8	30.53	nd
WC-03-QM19	9	31.18	85.7
KA-06-JQ17	10	31.87	27.9

^aCalculated as percentage of inhibition relative to controls vs. inhibitor concentration.

dimethyl-8-ribityllumazine, and treated with the indicated PABT compounds for 24 and 48 h. Indeed, the addition of exogenous riboflavin counteracts the effect of the inhibitors on bacterial growth after 48 h of treatment (Fig. 10A), while the supplementation with 6,7-dimethyl-8-ribityllumazine could not revert the bactericidal effect of the PABT compounds (Fig. 10B). Taking these results together, we conclude that the observed antibacterial effect of the PABT inhibitors on *B. abortus* can be attributed to their specific targeting of the RS enzyme.

RS inhibitors prevent intracellular *B. abortus* replication

In the search for effective antimicrobial agents against brucellosis, it is not enough to achieve bacterial inhibition in culture. Successful drugs should be able to penetrate the host cell to reach the intracellular growth niche of the pathogen. Thus, we subsequently measured the effect of the two most active compounds identified above (**4** and **10**) on the intracellular replication of *B. abortus*. For this purpose, we first established the nontoxic concentration ranges of inhibitors **4** and **10** on the J774A.1 cell line. In general, both compounds displayed a similar concentration dependent cytotoxicity effect, with concentrations above 30 μM producing death on most of the cultured cells, and no appreciable toxic effects at 10 μM (Fig. 11A). Thus, although these results indicate that there is a narrow working range, we still proceeded to test the efficacy of the compounds in intracellular *Brucella* infection assays. Remarkably, Fig. 11B shows that treatment of infected macrophages with 10 μM of

inhibitors **4** or **10** results in a significant reduction in viable intracellular bacteria (25 and 14-fold reduction, respectively). Therefore, inhibition of bacterial growth both in liquid and macrophage cultures indicate that the drug candidates **4** and **10** can efficiently cross the macrophage membrane, the *Brucella* intracellular niche and the bacterial membranes, to finally reach the cytoplasmic RS target.

Discussion

Targeting of metabolic pathways absent in mammals is an attractive strategy for the development of antibacterial therapeutic compounds. Histidine and branched-chain essential amino acid biosynthetic pathways have been targeted in *Brucella* spp. with some success [43,44]. Another example of enzymes targeted for anti-*Brucella* drug development corresponds to the carbonic anhydrases (CA). These enzymes are susceptible to selective inhibition over human CA II by a wide range of classical aromatic and heteroaromatic sulfonamides as well as carbohydrate-based compounds, affecting *Brucella* growth [45].

The riboflavin pathway is a very attractive target for antibiotic discovery since it is essential for the survival, intracellular trafficking and persistence of *B. abortus* [44]. Cushman and coworkers have reported the structure-based design and synthesis of several bacterial and fungal LS and RS antimetabolites with strong *in vitro* enzymatic inhibitory activity [27,29–33,36,46–51]. However, although these studies generated insight about these targets, most of the discovered compounds were hydrophilic and thus not suitable to penetrate cell membranes and exert their antibiotic activity.

A compound able to inhibit the growth of intracellular pathogens should pass through several membranes. Thus, is very important that the compounds assayed comply with the Lipinski rules to sustain a successful development pathway [52]. In consequence, a HTS approach using a library composed of compounds with drug-like properties is nowadays considered a very powerful and direct approach to find effective drug candidates against intracellular bacteria. In fact, a series of trifluoromethylated pyrazole compounds directed to RS with the capacity to inhibit the growth of both replicating and non-replicating *M. tuberculosis* were discovered using a commercial library HTS [37,53]. However, off-target effects on other bacterial enzymes such as *M. tuberculosis* CYP51, CYP121 and UDP-galactopyranose mutase could not be ruled out [54–56].

We have previously shown that riboflavin biosynthesis is essential for *Brucella* intracellular survival and

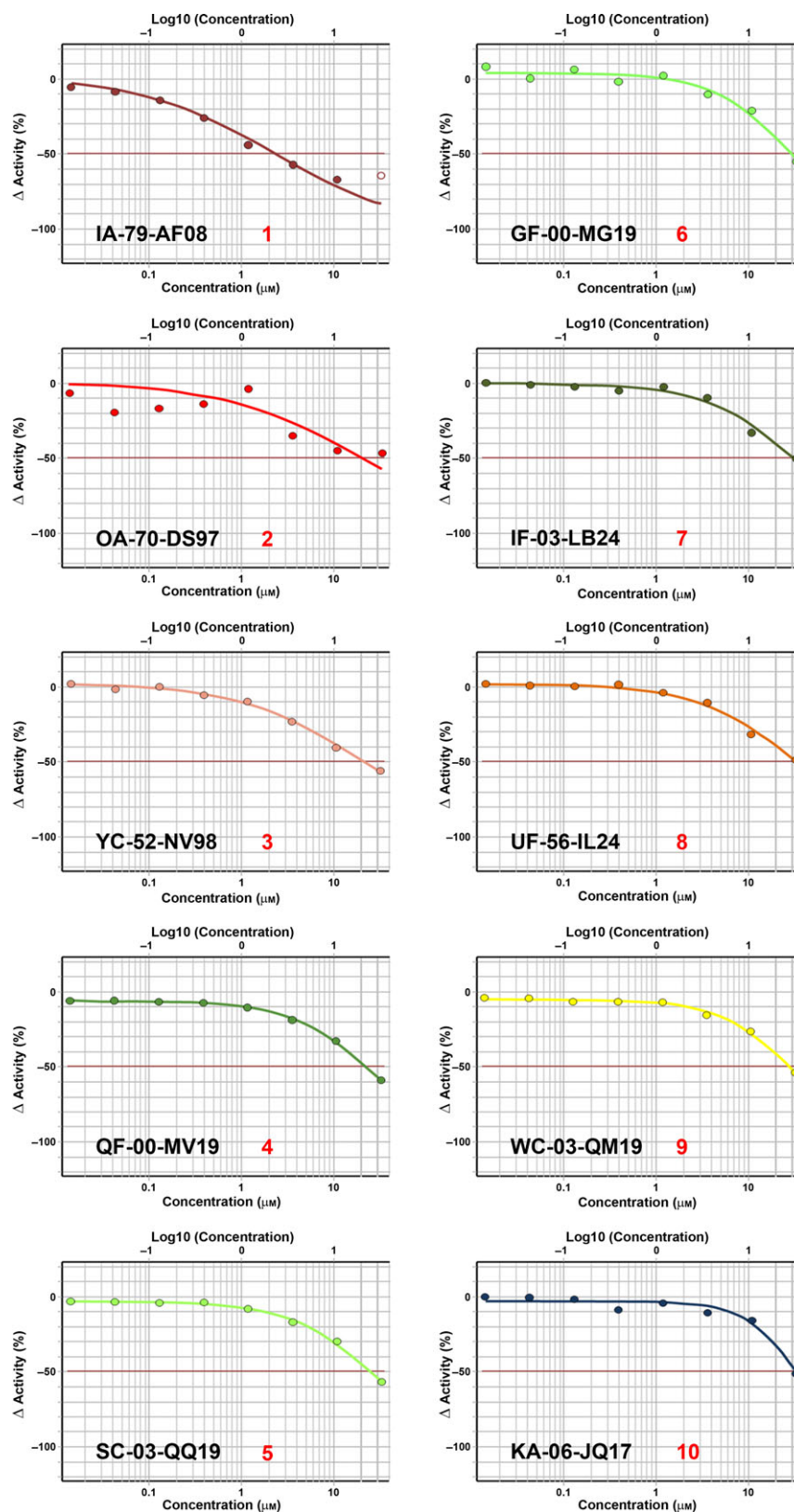


Fig. 6. Secondary screening of the selected hits against RS from *Brucella abortus*. Dose-response curves of the 10 compounds with the lowest IC_{50} values in the primary screening.

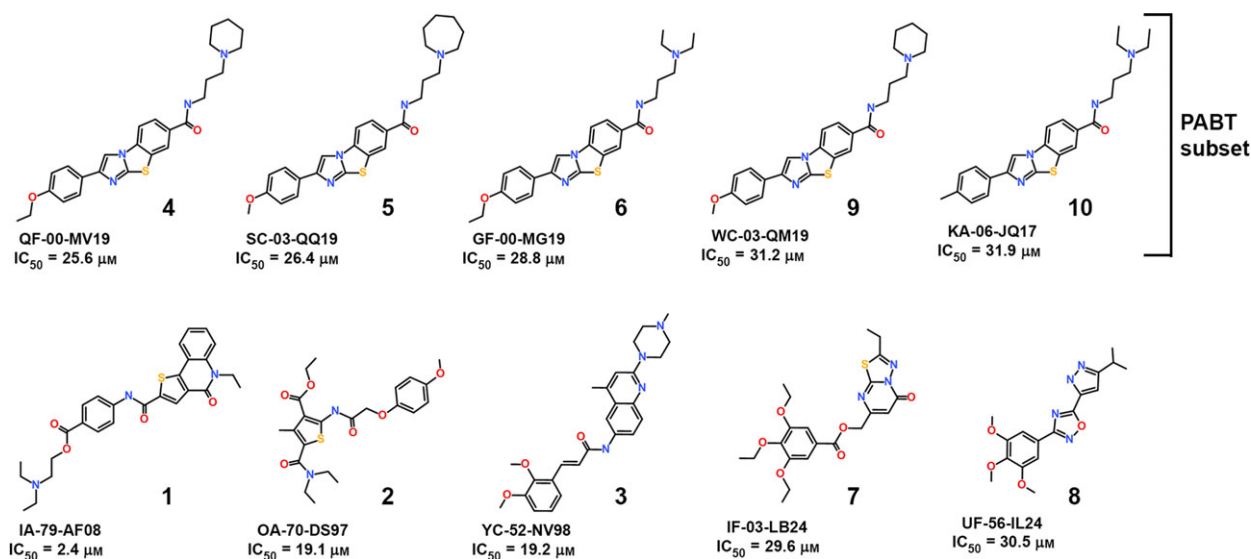


Fig. 7. Chemical structures of the 10 inhibitors with the lowest *in vitro* IC_{50} values against *Brucella abortus* RS. The molecules that share the same chemical PABT scaffold are located together in the upper row for clarity.



Fig. 8. The 2-PABT chemical scaffold. R1 corresponds to an alkyl or ethoxide substituent whereas R2 corresponds to an aliphatic tertiary amine.

replication in its niche, the brucellosome [14]. Thus, an ideal antibiotic to treat chronic brucellosis patients should attack bacteria in this reservoir, where *Brucella* can survive for decades. The present work summarizes the results obtained in a HTS by designing an automatable reaction to measure the RS inhibitory activity and using a large library with drug-like properties. This strategy allowed us to identify a family of compounds sharing a 2-PABT chemical scaffold, which showed inhibition of *Brucella* RS with IC_{50} values ranging from 2 to 30 μM . These IC_{50} values are in a similar range to the inhibition constants (K_i) described for some antimetabolites against RS and LS reported by Cushman and coworkers [28,31]. In addition, our RS inhibitors showed antimicrobial activity against *B. abortus* growth in culture, which was reverted by supplementing the medium with riboflavin, ruling out off-target effects. Most importantly, these compounds were further tested for antimicrobial activity in an *in vitro* infection model, demonstrating its antibiotic potential against mammalian intracellular pathogens.

These promising PABT hits can be further optimized. Based on our previous crystal structures of RS as apo-enzyme and in combination with different substrates and product analogues [26] and ongoing crystallization and NMR structural studies of RS : PABT complexes, we expect to develop structure-activity relationships (SAR) in order to direct the rational design of a lead compound. In particular, these studies may allow us to modify the R1 and R2 groups and/or the scaffold to (a) improve their complementarity to the RS active site; (b) make the compounds more effective to cross cellular membranes and reach the brucellosome; and (c) avoid bacterial efflux systems. SAR also can be used to decrease the toxicity of PABT hits for healthy cells.

An interesting point to discuss is the observation that adding riboflavin to the growth medium alleviates the antibacterial activity of the PABT compounds (Fig. 10A). This might suggest that these inhibitors could have reduced efficacy in individuals having an increased level of riboflavin in their diets. In a hypothetical scenario where an antibacterial drug was developed targeting the activity of *Brucella* RS, the extracellular riboflavin could in principle bypass this inhibition if it enters the bacterial cytosol. However, on the one hand *Brucella* does not code for riboflavin transporters and needs the vitamin to be in the extracellular medium at millimolar concentration to diffuse into the intracellular space [14]. On the other hand, the plasmatic concentration of riboflavin in humans lies at the nanomolar range [57] and the intracellular

Table 2. Physicochemical properties of the 10 compounds with the lowest IC₅₀ values against *Brucella abortus* RS enzymatic activity.

Compound commercial name	Compound number	MW (Da)	clogP	HBA (sum of N and O atoms)	HBD (sum of OH and NH groups)	tPSA (Å ²)	nRot	PABT subset
IA-79-AF08	1	491.6	4.57	5	1	107.2	10	NO
OA-70-DS97	2	448.5	3.53	6	1	122.4	11	NO
YC-52-NV98	3	446.5	3.95	6	1	66.9	6	NO
QF-00-MV19	4	462.6	4.71	4	1	87.1	8	YES
SC-03-QQ19	5	462.6	4.68	4	1	87.1	7	YES
GF-00-MG19	6	450.6	4.94	4	1	87.1	10	YES
IF-03-LB24	7	447.5	3.72	9	0	124.3	11	NO
UF-56-IL24	8	330.3	3.24	1	7	95.3	6	NO
WC-03-QM19	9	448.6	4.37	4	1	87.1	7	YES
KA-06-JQ17	10	420.6	4.73	3	1	77.9	8	YES

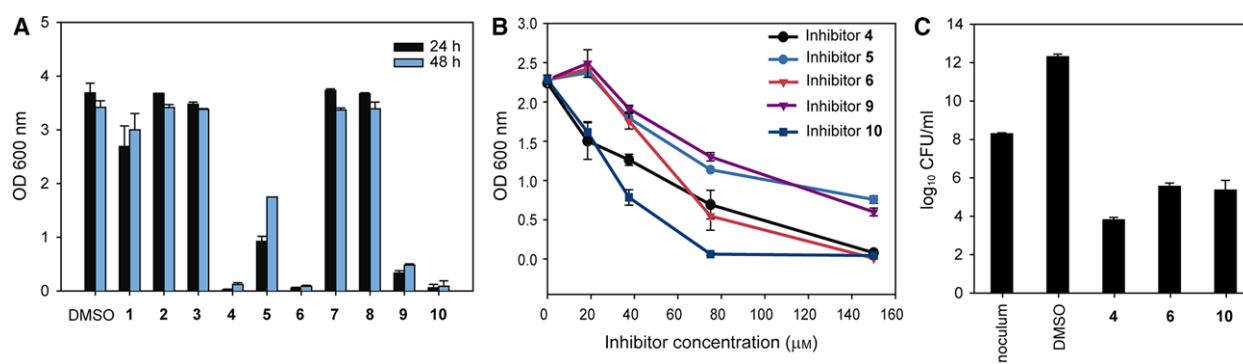


Fig. 9. Effect of the RS inhibitors on *Brucella abortus* growth. (A) Susceptibility of *B. abortus* to the ten selected compounds in TSB cultures. *Brucella abortus* at OD₆₀₀ = 0.01 were treated with the compounds (150 μM) for 24 and 48 h. Control: DMSO. (B) Dose–response effect of the PABT series of RS inhibitors on *B. abortus* cultured in TSB. Bacterial cultures were treated with increasing concentrations of the inhibitors for 24 h. (C) Bactericidal effect of the PABT RS inhibitors. Cultures of *B. abortus* at OD₆₀₀ = 0.01 were treated with the indicated compounds (150 μM) and the CFUs determined at *t* = 0 and 24 h, with DMSO as control. Each experiment from panels (A–C) was performed independently at least three times, and the result of one representative experiment is shown. Values represent the mean ± SD.

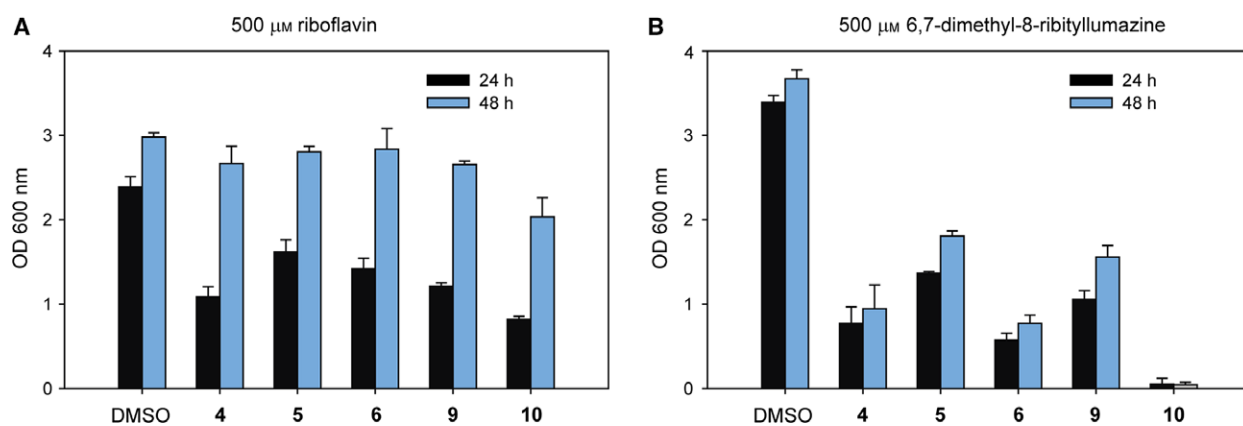


Fig. 10. *In vivo* RS specific targeting by the PABT compounds. Susceptibility of *Brucella abortus* to the selected RS inhibitors in TSB cultures supplemented with 500 μM of (A) riboflavin or (B) 6,7-dimethyl-8-ribityllumazine and treated with indicated inhibitors (150 μM) for 24 and 48 h. DMSO was used as control. The means ± SD of technical triplicates of one representative experiment out of two performed are presented.

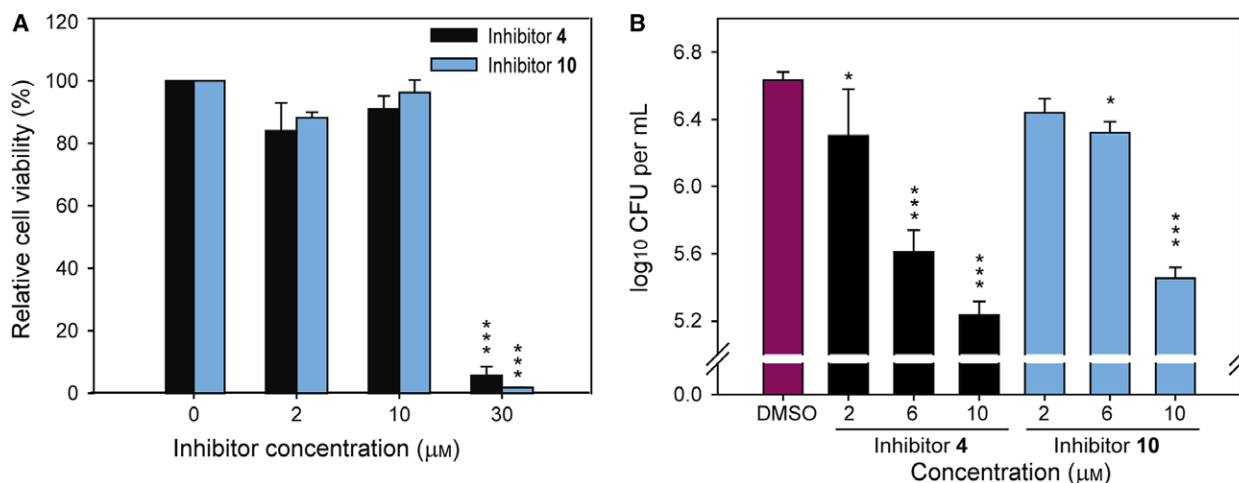


Fig. 11. Inhibition of *Brucella* macrophages infection by compounds **4** and **10**. (A) Cytotoxic activity assay of the RS inhibitors on murine macrophagic J774.1 cells. For this experiment, cells were treated with increasing concentrations of compounds **4** and **10** for 24 h, and then cell viability was determined by the Trypan Blue exclusion assay. Values represent percent mean \pm SD, relative to the control treatment without inhibitor ($n = 3$). (B) Efficacy of the inhibitors **4** and **10** against intracellular *Brucella* infection. At 24 h post infection, J774.A1 cells were treated with 2, 6 and 10 μ M of compounds **4** or **10**. After a 24 h treatment, cells were washed, lysed and *Brucella abortus* CFU were determined. Values represent the mean \pm SD of two independent experiments and are expressed as the logarithm of the CFU of intracellular bacteria per ml. The statistical analysis was performed by a one-way ANOVA followed by a Bonferroni's post hoc test ($*P < 0.01$, $***P < 0.001$), comparing each condition with respect to the control.

concentration is even lower, in attomolar quantities [58]. Increasing the riboflavin intake in the diet could eventually lead to an increase in its plasmatic level yet remaining below the micromolar range [59]. Therefore, during a hypothetical anti-brucellosis treatment with RS inhibitor drugs, the riboflavin concentration inside the host is not expected to allow the bacteria to live neither in plasma nor inside the host cells.

In summary, we have performed a HTS and found several compounds that are effective inhibitors of *B. abortus* RS. We have demonstrated that five of these compounds are biologically active against *Brucella* by inhibiting its growth in culture, with two of them also inhibiting bacterial growth within the host cell. Taken together, our data suggest that RS from *B. abortus* constitutes a suitable target for alternative antibacterial therapy, notably against strains resistant to conventional antibiotic treatments. Finally, as RS is highly conserved across pathogenic microorganisms, the potential application of the compounds reported here might also be effective for other infectious diseases.

Materials and methods

Chemicals and biological reagents

Riboflavin, β -Glycerophosphate disodium salt hydrate, BSA fraction V 96%, Sodium orthovanadate (Na_3VO_4), HEPES and DTT were purchased from Sigma–Aldrich (St. Louis,

MO, USA). Coating reagents CR-3 and CR-8 were purchased from Caliper Life Sciences (Hopkinton, MA, USA). Tween 20 was purchased from Bio-Rad (Hercules, CA, USA) and trifluoroacetic acid (TFA) from Pierce (Dallas, TX, USA). 30% Aqueous Solution BRIJ 35 was purchased from Calbiochem (San Diego, CA, USA). The 5-carboxyfluorescein labeled peptide JAK3 (122.6 kDa) was obtained from Biosyntan GmbH (Berlin, Germany) and the 6,7-dimethyl-8-ribitylumazine substrate (326 Da) was kindly provided by M. Fischer from the University of Hamburg, Germany.

RS expression and purification

RS from *B. abortus* (69 kDa) was expressed and purified as described previously [26]. In short, the protein was expressed in *Escherichia coli* BL21(DE3) cells (Stratagene, San Diego, CA, USA) and purified by affinity chromatography with a HisTrap HP column followed by a size exclusion chromatography step in a Superdex 200 column (all columns from GE Healthcare, Chicago, IL, USA). Fractions corresponding to the protein were pooled, concentrated to 60 $\text{mg}\cdot\text{mL}^{-1}$ in 10 mM Tris, 25 mM sodium chloride, pH 7.4, and stored at -80°C until use.

Mobility shift-based screening assay (MSA)

The MSA was performed on a Caliper LabChip 3000 Drug Discovery instrument (Caliper Life Sciences, Waltham, MA, USA) in an off-chip mode. The reaction buffer contained 50 mM HEPES, 0.02% Tween 20, 1 mM DTT, 0.02%

BSA, 10 μM Na_3VO_4 , and 10 mM β -Glycerophosphate, pH 7.5. The NIBR Drug Discovery Incubator library for external collaborations comprises 44 000 pure chemical compounds accessible from the Hit Finding Unit of Novartis Pharma AG (Basel, Switzerland). The compounds were selected according to their chemical diversity and drug-like properties, and their purity was assessed by LC-MS (data not shown). A quantity of 90 nL of the compound stock solutions [at 10 mM in 90% (v/v) DMSO/water] was placed in a 384-well assay microtiter plate (Corning Inc., Corning, NY, USA) prior to the addition of 4.5 μL of RS (16 nM) and the fluorescent peptide JAK3 (400 nM) in 1 \times reaction buffer. Subsequently, 4.5 μL of the 6,7-dimethyl-8-ribityllumazine substrate at 40 μM in 1 \times reaction buffer were added. The final compound concentration was 30 μM and the DMSO concentration was 0.9% (v/v). The microtiter plates with the assay solution were incubated for 60 min at 30 $^\circ\text{C}$ and 95% humidity, prior to the addition of 1.2% (v/v) TFA/buffer solution to stop the enzymatic reaction. The assay plate was subjected to the Caliper LabChip 3000 reader, equipped with a 12-sipper chip. The reaction mixture was sampled for 1 s for electrophoretic separation of the 6,7-dimethyl-8-ribityllumazine and riboflavin peaks at a pressure of -2.1 psi and an upstream voltage of -750 V and a downstream voltage of -2500 V.

The Caliper technology requires a standardization of the runtime and peak height. For this purpose, the 5-carboxyfluorescein labeled peptide JAK3 (a reference dye successfully applied in previous HTS experiments at Novartis) was used as an internal standard ($\lambda_{\text{excitation}} = 493$ nm, $\lambda_{\text{emission}} = 517$ nm).

The conversion rate (r) was defined as the height of the product peak divided by the sum of the peak heights from product and substrate. The effect of a test compound on the enzymatic reaction was quantified using the Novartis proprietary software package HELIOS (Novartis, Basel, Switzerland). The inhibition percentage was calculated relative to the high and low controls as:

$$\% \text{Inhibition} = 100 \times \left(1 - \frac{(r - r_{\text{low control}})}{(r_{\text{high control}} - r_{\text{low control}})} \right)$$

where the low controls corresponded to 100% inhibition the presence of 5.5% TFA and the high controls to the absence of inhibitor compounds.

The quality of the assay was assessed by calculating the Z' factor value using the following equation: [60]

$$Z' = 1 - \frac{((3\text{SD of high control}) + (3\text{SD of low control}))}{|(\text{mean of high control} - \text{mean of low control})|}$$

Validation of screening hits by 50% inhibitory concentrations (IC_{50}) values

IC_{50} values for selected primary screening hits were determined from dose–response curves. Typically, reactions were

performed in 384-well microtiter plates in reaction buffer at 0.008 μM RS and eight concentrations of the compounds (0.015–32 μM). The IC_{50} values were calculated from the plot of percentage of inhibition relative to controls vs. inhibitor concentration by a logistics fit using the HELIOS software.

Bacterial growth conditions

Brucella abortus 2308 strain cells were grown in TSB or on tryptic soy agar plates at 37 $^\circ\text{C}$, on a rotary shaker (200 r.p.m.) or incubator, respectively. All work with viable *B. abortus* was performed on a biosafety level 3 laboratory.

Susceptibility of *B. abortus* to the RS inhibitor compounds

RS inhibitor compounds were dissolved in DMSO at a final concentration of 20 mM prior to use. The determination of the susceptibility of *B. abortus* to these compounds was carried out by measuring the optical density at 600 nm (OD_{600}) of treated liquid cultures as a function of time compared to a control (DMSO only treatment). Overnight cultures were diluted in TSB at $\text{OD}_{600} = 0.01$, then the individual inhibitors were added to a final concentration of 150 μM and the resulting OD_{600} were measured at 24 and 48 h postincubation. When indicated, the cultures were diluted in TSB supplemented with 500 μM of riboflavin or 6,7-dimethyl-8-ribityllumazine.

To perform the dose–response assays of the inhibitors **4**, **5**, **6**, **9**, and **10**, *B. abortus* cultures were diluted to $\text{OD}_{600} = 0.01$ and incubated with 2-fold serial dilutions of the indicated compounds. Optical densities were measured 24 h later. Bacterial viability of cultures treated with the compounds **4**, **6**, and **10** for 24 h was assessed by plating serial dilutions of *B. abortus* cultures and counting the resulting CFU 24 h later. Cultures incubated with DMSO were used as control.

Macrophage toxicity assay

Murine macrophage-like cells J774A.1 (ATCC, Manassas, VA, USA) were seeded at a density of 1.5×10^5 cells per well in 24-well plates (Corning) with Dulbecco's modified Eagle's medium (DMEM) and 10% FBS (Gibco, Waltham, MA, USA) at 37 $^\circ\text{C}$ under 5% CO_2 24 h prior to treatment. Thereafter, the macrophage cells were incubated with 2, 10 and 30 μM of inhibitors **4** or **10** for another 24 h under similar conditions. Cell viability was measured by counting the number of viable cells after Trypan blue staining using a gridded hemocytometer. In all cases, at least 100 cells were counted to determine the percentage of live cells. Assays were performed in duplicate wells. The results represent the averages from at least three independent experiments.

Infection of J774A.1 cells

Murine macrophage-like J774A.1 cells were plated at a density of 1.5×10^5 cells per well in 24-well plates and grown in DMEM added with 10% FBS for 24 h at 37 °C and 5% CO₂ prior to the infection. Then, cells were infected with *B. abortus* in triplicate wells at a 100 : 1 multiplicity of infection. After 1 h, cells were washed with PBS and incubated with DMEM added with 25 µg mL⁻¹ gentamicin. After 1 h (time 0), the monolayers were washed with DMEM and incubated for another 24 h with complete medium containing 10 µg mL⁻¹ gentamicin with the addition of 2, 6 or 10 µM of inhibitors **4** or **10**. Thereafter, the infected macrophages were washed with PBS and lysed with 0.1% Triton X-100 (Sigma-Aldrich). Intracellular *B. abortus* CFUs were determined by plating serial dilutions of the lysates and counting the bacterial colonies after 24 h of incubation. The results represent the average ratio between the CFU per mL obtained from the treated wells and the control wells, which were incubated only with DMSO.

Statistical analysis

Statistical analyses were performed with One-way ANOVA with a Bonferroni's multiple comparison post hoc test using GRAPHPAD PRISM5 (GraphPad Software, San Diego, CA, USA). Data are presented as mean ± standard deviation (SD). *P*-values of 0.05 or lower were considered as significant. Statistical significance levels were defined as follows: **P* < 0.05; ***P* < 0.01; ****P* < 0.001.

Acknowledgements

This work was supported by the Argentinian Research Council (CONICET) and the Argentinian Agency for Scientific and Technological Development (ANPCyT) through the research grant PICT 2014-0959. We acknowledge Novartis for the participation of MIS in the Next Generation Scientist Program in Basel, Switzerland.

Conflicts of interest

The authors declare no conflicts of interest.

Author contributions

JT and FAG conceived and supervised the study; MIS, MdCC, SLR, and MLC performed experiments; all authors analyzed data and wrote the manuscript.

References

- Godfroid J, Cloeckeaert A, Liautard JP, Kohler S, Fretin D, Walravens K, Garin-Bastuji B & Letesson JJ

- (2005) From the discovery of the Malta fever's agent to the discovery of a marine mammal reservoir, brucellosis has continuously been a re-emerging zoonosis. *Vet Res* **36**, 313–326.
- Pappas G, Akritidis N, Bosilkovski M & Tsianos E (2005) Brucellosis. *N Engl J Med* **352**, 2325–2336.
- Gorvel JP (2008) Brucella: a Mr “Hide” converted into Dr Jekyll. *Microbes Infect* **10**, 1010–1013.
- Franc KA, Krecek RC, Hasler BN & Arenas-Gamboa AM (2018) Brucellosis remains a neglected disease in the developing world: a call for interdisciplinary action. *BMC Public Health* **18**, 125.
- Pappas G, Papadimitriou P, Akritidis N, Christou L & Tsianos EV (2006) The new global map of human brucellosis. *Lancet Infect Dis* **6**, 91–99.
- Ariza J, Bosilkovski M, Cascio A, Colmenero JD, Corbel MJ, Falagas ME, Memish ZA, Roushan MR, Rubinstein E, Sipsas NV *et al.* (2007) Perspectives for the treatment of brucellosis in the 21st century: the Ioannina recommendations. *PLoS Med* **4**, e317.
- Yousefi-Nooraie R, Mortaz-Hejri S, Mehrani M & Sadeghipour P (2012) Antibiotics for treating human brucellosis. *Cochrane Database Syst Rev* **10**, CD007179.
- Solis Garcia del Pozo J & Solera J (2012) Systematic review and meta-analysis of randomized clinical trials in the treatment of human brucellosis. *PLoS ONE* **7**, e32090.
- Bacher A, Eberhardt S, Fischer M, Kis K & Richter G (2000) Biosynthesis of vitamin b2 (riboflavin). *Annu Rev Nutr* **20**, 153–167.
- Joosten V & van Berkel WJ (2007) Flavoenzymes. *Curr Opin Chem Biol* **11**, 195–202.
- Long Q, Ji L, Wang H & Xie J (2010) Riboflavin biosynthetic and regulatory factors as potential novel anti-infective drug targets. *Chem Biol Drug Des* **75**, 339–347.
- Morgunova E, Illarionov B, Sambaiah T, Haase I, Bacher A, Cushman M, Fischer M & Ladenstein R (2006) Structural and thermodynamic insights into the binding mode of five novel inhibitors of lumazine synthase from *Mycobacterium tuberculosis*. *FEBS J* **273**, 4790–4804.
- Rollenhagen C & Bumann D (2006) Salmonella enterica highly expressed genes are disease specific. *Infect Immun* **74**, 1649–1660.
- Bonomi HR, Marchesini MI, Klinke S, Ugalde JE, Zylberman V, Ugalde RA, Comerci DJ & Goldbaum FA (2010) An atypical riboflavin pathway is essential for *Brucella abortus* virulence. *PLoS ONE* **5**, e9435.
- Garcia Angulo VA, Bonomi HR, Posadas DM, Serer MI, Torres AG, Zorreguieta A & Goldbaum FA (2013) Identification and characterization of RibN, a novel family of riboflavin transporters from *Rhizobium leguminosarum* and other proteobacteria. *J Bacteriol* **195**, 4611–4619.

- 16 Gutierrez-Preciado A, Torres AG, Merino E, Bonomi HR, Goldbaum FA & Garcia-Angulo VA (2015) Extensive identification of bacterial riboflavin transporters and their distribution across bacterial species. *PLoS ONE* **10**, e0126124.
- 17 Fischer M & Bacher A (2008) Biosynthesis of vitamin B₂: structure and mechanism of riboflavin synthase. *Arch Biochem Biophys* **474**, 252–265.
- 18 Fischer M, Romisch W, Illarionov B, Eisenreich W & Bacher A (2005) Structures and reaction mechanisms of riboflavin synthases of eubacterial and archaeal origin. *Biochem Soc Trans* **33**, 780–784.
- 19 Fischer M & Bacher A (2005) Biosynthesis of flavocoenzymes. *Nat Prod Rep* **22**, 324–350.
- 20 Klinke S, Zylberman V, Vega DR, Guimaraes BG, Braden BC & Goldbaum FA (2005) Crystallographic studies on decameric *Brucella* spp. lumazine synthase: a novel quaternary arrangement evolved for a new function? *J Mol Biol* **353**, 124–137.
- 21 Zylberman V, Craig PO, Klinke S, Braden BC, Cauerhff A & Goldbaum FA (2004) High order quaternary arrangement confers increased structural stability to *Brucella* sp. lumazine synthase. *J Biol Chem* **279**, 8093–8101.
- 22 Berguer PM, Mundinano J, Piazzon I & Goldbaum FA (2006) A polymeric bacterial protein activates dendritic cells via TLR4. *J Immunol* **176**, 2366–2372.
- 23 Craig PO, Alzogaray V & Goldbaum FA (2012) Polymeric display of proteins through high affinity leucine zipper peptide adaptors. *Biomacromol* **13**, 1112–1121.
- 24 Laplagne DA, Zylberman V, Ainciart N, Steward MW, Sciotto E, Fossati CA & Goldbaum FA (2004) Engineering of a polymeric bacterial protein as a scaffold for the multiple display of peptides. *Proteins* **57**, 820–828.
- 25 Yang Y, Wang L, Yin J, Wang X, Cheng S, Lang X, Wang X, Qu H, Sun C, Wang J *et al.* (2011) Immunoproteomic analysis of *Brucella melitensis* and identification of a new immunogenic candidate protein for the development of brucellosis subunit vaccine. *Mol Immunol* **49**, 175–184.
- 26 Serer MI, Bonomi HR, Guimaraes BG, Rossi RC, Goldbaum FA & Klinke S (2014) Crystallographic and kinetic study of riboflavin synthase from *Brucella abortus*, a chemotherapeutic target with an enhanced intrinsic flexibility. *Acta Crystallogr D Biol Crystallogr* **70**, 1419–1434.
- 27 Cushman M, Mavandadi F, Kugelbrey K & Bacher A (1998) Synthesis of 2,6-dioxo-(1H,3H)-9-N-ribityl-purine and 2,6-dioxo-(1H,3H)-8-aza-9-N-ribityl-purine as inhibitors of lumazine synthase and riboflavin synthase. *Bioorg Med Chem* **6**, 409–415.
- 28 Cushman M, Yang D, Kis K & Bacher A (2001) Design, synthesis, and evaluation of 9-D-ribityl-1,3,7-trihydro-2,6,8-purinetrione, a potent inhibitor of riboflavin synthase and lumazine synthase. *J Org Chem* **66**, 8320–8327.
- 29 Cushman M, Jin G, Sambaiah T, Illarionov B, Fischer M, Ladenstein R & Bacher A (2005) Design, synthesis, and biochemical evaluation of 1,5,6,7-tetrahydro-6,7-dioxo-9-D-ribitylaminolumazines bearing alkyl phosphate substituents as inhibitors of lumazine synthase and riboflavin synthase. *J Org Chem* **70**, 8162–8170.
- 30 Cushman M, Sambaiah T, Jin G, Illarionov B, Fischer M & Bacher A (2004) Design, synthesis, and evaluation of 9-D-ribitylamino-1,3,7,9-tetrahydro-2,6,8-purinetriones bearing alkyl phosphate and alpha, alpha-difluorophosphonate substituents as inhibitors of riboflavin synthase and lumazine synthase. *J Org Chem* **69**, 601–612.
- 31 Cushman M, Yang D, Gerhardt S, Huber R, Fischer M, Kis K & Bacher A (2002) Design, synthesis, and evaluation of 6-carboxyalkyl and 6-phosphonoxyalkyl derivatives of 7-oxo-8-ribitylaminolumazines as inhibitors of riboflavin synthase and lumazine synthase. *J Org Chem* **67**, 5807–5816.
- 32 Scheuring J, Fischer M, Cushman M, Lee J, Bacher A & Oschkinat H (1996) NMR analysis of site-specific ligand binding in oligomeric proteins. Dynamic studies on the interaction of riboflavin synthase with trifluoromethyl-substituted intermediates. *Biochemistry* **35**, 9637–9646.
- 33 Scheuring J, Lee J, Cushman M, Patel H, Patrick DA & Bacher A (1994) (Trifluoromethyl)lumazine derivatives as 19F NMR probes for lumazine protein. *Biochemistry* **33**, 7634–7640.
- 34 Chen J, Sambaiah T, Illarionov B, Fischer M, Bacher A & Cushman M (2004) Design, synthesis, and evaluation of acyclic C-nucleoside and N-methylated derivatives of the ribitylaminopyrimidine substrate of lumazine synthase as potential enzyme inhibitors and mechanistic probes. *J Org Chem* **69**, 6996–7003.
- 35 Zhang Y, Illarionov B, Bacher A, Fischer M, Georg GI, Ye QZ, Vander Velde D, Fanwick PE, Song Y & Cushman M (2007) A novel lumazine synthase inhibitor derived from oxidation of 1,3,6,8-tetrahydroxy-2,7-naphthyridine to a tetraazapyrenehexaone derivative. *J Org Chem* **72**, 2769–2776.
- 36 Talukdar A, Illarionov B, Bacher A, Fischer M & Cushman M (2007) Synthesis and enzyme inhibitory activity of the s-nucleoside analogue of the ribitylaminopyrimidine substrate of lumazine synthase and product of riboflavin synthase. *J Org Chem* **72**, 7167–7175.
- 37 Zhao Y, Bacher A, Illarionov B, Fischer M, Georg G, Ye QZ, Fanwick PE, Franzblau SG, Wan B & Cushman M (2009) Discovery and development of the covalent hydrates of trifluoromethylated pyrazoles as riboflavin synthase inhibitors with antibiotic activity against *Mycobacterium tuberculosis*. *J Org Chem* **74**, 5297–5303.

- 38 Lipinski CA, Lombardo F, Dominy BW & Feeney PJ (2001) Experimental and computational approaches to estimate solubility and permeability in drug discovery and development settings. *Adv Drug Deliv Rev* **46**, 3–26.
- 39 Veber DF, Johnson SR, Cheng HY, Smith BR, Ward KW & Kopple KD (2002) Molecular properties that influence the oral bioavailability of drug candidates. *J Med Chem* **45**, 2615–2623.
- 40 Camenisch G, Folkers G & van de Waterbeemd H (1996) Review of theoretical passive drug absorption models: historical background, recent developments and limitations. *Pharm Acta Helv* **71**, 309–327.
- 41 Ertl P, Rohde B & Selzer P (2000) Fast calculation of molecular polar surface area as a sum of fragment-based contributions and its application to the prediction of drug transport properties. *J Med Chem* **43**, 3714–3717.
- 42 Artursson Per BCAS (2004) Intestinal Absorption: the Role of Polar Surface Area. In *Drug Bioavailability: Estimation of Solubility, Permeability, Absorption and Bioavailability* (Han van de Waterbeemd HL & Artursson P eds), pp. 53–83. Wiley-VCH, Weinheim, Germany.
- 43 Joseph P, Abdo MR, Boegegrain RA, Montero JL, Winum JY & Kohler S (2007) Targeting of the *Brucella suis* virulence factor histidinol dehydrogenase by histidinol analogues results in inhibition of intramacrophagic multiplication of the pathogen. *Antimicrob Agents Chemother* **51**, 3752–3755.
- 44 Boegegrain RA, Liautard JP & Kohler S (2005) Targeting of the virulence factor acetohydroxyacid synthase by sulfonyleureas results in inhibition of intramacrophagic multiplication of *Brucella suis*. *Antimicrob Agents Chemother* **49**, 3922–3925.
- 45 Kohler S, Ouahrani-Bettache S & Winum JY (2017) *Brucella suis* carbonic anhydrases and their inhibitors: towards alternative antibiotics? *J Enzyme Inhib Med Chem* **32**, 683–687.
- 46 Cushman M, Mavandadi F, Yang D, Kugelbrey K, Kis K & Bacher A (1999) Synthesis and biochemical evaluation of Bis(6,7-dimethyl-8-D-ribityllumazines) as potential bisubstrate analogue inhibitors of riboflavin synthase. *J Org Chem* **64**, 4635–4642.
- 47 Cushman M, Mihalic JT, Kis K & Bacher A (1999) Design and synthesis of 6-(6-D-ribitylamino-2,4-dihydroxypyrimidin-5-yl)-1-hexyl phosphonic acid, a potent inhibitor of lumazine synthase. *Bioorg Med Chem Lett* **9**, 39–42.
- 48 Zhang Y, Jin G, Illarionov B, Bacher A, Fischer M & Cushman M (2007) A new series of 3-alkyl phosphate derivatives of 4,5,6,7-tetrahydro-1-D-ribityl-1H-pyrazolo[3,4-d]pyrimidinedione as inhibitors of lumazine synthase: design, synthesis, and evaluation. *J Org Chem* **72**, 7176–7184.
- 49 Illarionov B, Kemter K, Eberhardt S, Richter G, Cushman M & Bacher A (2001) Riboflavin synthase of *Escherichia coli*. Effect of single amino acid substitutions on reaction rate and ligand binding properties. *J Biol Chem* **276**, 11524–11530.
- 50 Zhang Y, Illarionov B, Morgunova E, Jin G, Bacher A, Fischer M, Ladenstein R & Cushman M (2008) A new series of N-[2,4-dioxo-6-d-ribitylamino-1,2,3,4-tetrahydropyrimidin-5-yl]oxalamic acid derivatives as inhibitors of lumazine synthase and riboflavin synthase: design, synthesis, biochemical evaluation, crystallography, and mechanistic implications. *J Org Chem* **73**, 2715–2724.
- 51 Harvey RA & Plaut GW (1966) Riboflavin synthetase from yeast. Properties of complexes of the enzyme with lumazine derivatives and riboflavin. *J Biol Chem* **241**, 2120–2136.
- 52 Lipinski CA (2004) Lead- and drug-like compounds: the rule-of-five revolution. *Drug Discov Today Technol* **1**, 337–341.
- 53 Kaiser J, Illarionov B, Rohdich F, Eisenreich W, Saller S, den Brulle JV, Cushman M, Bacher A & Fischer M (2007) A high-throughput screening platform for inhibitors of the riboflavin biosynthesis pathway. *Anal Biochem* **365**, 52–61.
- 54 McLean KJ, Marshall KR, Richmond A, Hunter IS, Fowler K, Kieser T, Gurcha SS, Besra GS & Munro AW (2002) Azole antifungals are potent inhibitors of cytochrome P450 mono-oxygenases and bacterial growth in mycobacteria and streptomycetes. *Microbiology* **148**, 2937–2949.
- 55 Menozzi G, Merello L, Fossa P, Schenone S, Ranise A, Mosti L, Bondavalli F, Loddo R, Murgioni C, Mascia V *et al.* (2004) Synthesis, antimicrobial activity and molecular modeling studies of halogenated 4-[1H-imidazol-1-yl(phenyl)methyl]-1,5-diphenyl-1H-pyrazoles. *Bioorg Med Chem* **12**, 5465–5483.
- 56 Carlson EE, May JF & Kiessling LL (2006) Chemical probes of UDP-galactopyranose mutase. *Chem Biol* **13**, 825–837.
- 57 Eussen SJ, Vollset SE, Hustad S, Midttun O, Meyer K, Fredriksen A, Ueland PM, Jenab M, Slimani N, Boffetta P *et al.* (2010) Plasma vitamins B2, B6, and B12, and related genetic variants as predictors of colorectal cancer risk. *Cancer Epidemiol Biomarkers Prev* **19**, 2549–2561.
- 58 Huhner J, Ingles-Prieto A, Neuss C, Lammerhofer M & Janovjak H (2015) Quantification of riboflavin, flavin mononucleotide, and flavin adenine dinucleotide in mammalian model cells by CE with LED-induced fluorescence detection. *Electrophoresis* **36**, 518–525.
- 59 Zemleni J, Galloway JR & McCormick DB (1996) Pharmacokinetics of orally and intravenously administered riboflavin in healthy humans. *Am J Clin Nutr* **63**, 54–66.
- 60 Zhang JH, Chung TD & Oldenburg KR (1999) A simple statistical parameter for use in evaluation and validation of high throughput screening assays. *J Biomol Screen* **4**, 67–73.